Acta Crystallographica Section F
Structural Biology and Crystallization Communications
ISSN 1744-3091

Purification, crystallization and preliminary X-ray diffraction analysis of an oomycete-derived Nep1-like protein

Borries Luberacki,[a]‡§ Michael Weyand,[b]§ Ulrich Seitz,[a] Wolfgang Koch,[a] Claudia Oecking[a] and Christian Ottmann[a,b]*

[a]Center for Plant Molecular Biology, Auf der Morgenstelle 5, 72076 Tübingen, Universität Tübingen, Germany, and [b]Chemical Genomics Centre, Otto-Hahn-Strasse 15, 44227 Dortmund, Germany

‡ Present address: GMI – Gregor Mendel Institute of Molecular Plant Biology GmbH, Dr Bohr-Gasse 3, 1030 Vienna, Austria.
§ These authors contributed equally.

Correspondence e-mail: christian.ottmann@cgc.mpg.de

Received 29 August 2008
Accepted 13 November 2008

The elicitor protein Nep1-like protein from the plant pathogen *Pythium aphanidermatum* was purified and crystallized using the hanging-drop vapour-diffusion method. A native data set was collected to 1.35 Å resolution at 100 K using synchrotron radiation. Since selenomethionine-labelled protein did not crystallize under the original conditions, a second crystal form was identified that yielded crystals that diffracted to 2.1 Å resolution. A multiple-wavelength anomalous dispersion (MAD) experiment was performed at 100 K and all four selenium sites were identified, which allowed solution of the structure.

1. Introduction

Plants, like animals, have developed molecular mechanisms to distinguish self from non-self in order to resist infection by pathogens. The primary immune response depends on the recognition of so-called pathogen-associated molecular patterns (PAMPs; Chisholm *et al.*, 2006). In plants, such PAMPs have long been known as elicitors that counteract infection by activating defence responses in the host (Nürnberger *et al.*, 2004). Probably the most prominent example of a protein elicitor implicated in plant immune responses is flg22, a 22-amino-acid peptide derived from bacterial flagellin which induces the expression of numerous defence-related genes (Zipfel *et al.*, 2004). In a recent study, it was shown that the spectrum of Nep1-like protein-triggered immune responses in the model plant *Arabidopsis thaliana* resembles that of flg22 (Qutob *et al.*, 2006).

The first protein of this family, discovered in 1995, was Nep1 (necrosis- and ethylene-inducing peptide 1), a 24 kDa protein that was isolated from culture filtrates of the phytopathogenic fungus *Fusarium oxysporum* (Bailey, 1995). All subsequently discovered proteins of this family were called NLPs (Nep1-like proteins).

NLPs are found in bacteria, fungi and oomycetes. They share a high degree of sequence similarity and induce the so-called hypersensitive response (a programmed cell death serving to confine sites of infection) in more than 20 dicotyledonous plants (Gijzen & Nürnberger, 2006). In addition to their role as eliciting molecules, they seem to enhance the virulence of necrotrophic pathogens. For example, overexpression of Nep1 in a hypovirulent fungus increases disease symptoms in the respective host plant (Amsellem *et al.*, 2002), whereas loss of NLP expression in the bacterial pathogen *Erwinia carotovora* results in decreased aggressiveness towards potato (Mattinen *et al.*, 2004). The cell death-inducing activity of NLPs and their wide activity spectrum are reminiscent of cytolytic toxins. Altogether this led to the classification of NLPs as both elicitor-like molecules and toxin-like virulence factors (Qutob *et al.*, 2006).

Since no structure is available of this important family of proteins, the 213-amino-acid NLP from *Pythium aphanidermatum* (NLP_{Pya}) and its SeMet-labelled derivative were overexpressed in *Escherichia coli*, purified and crystallized in order to solve the structure by MAD phasing.

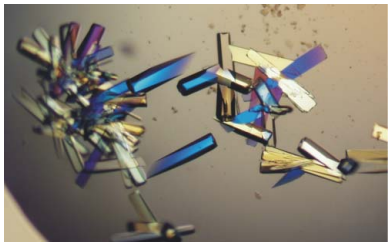

2. Methods and results

2.1. Overexpression and purification

NLP_{Pya} (Qutob *et al.*, 2006), formerly called $PaNie_{213}$ (Veit *et al.*, 2001), was overexpressed and purified as reported previously (Veit *et al.*, 2001) with slight modifications. In order to express the functional full-length protein devoid of its eukaryotic secretory signal sequence in bacteria, an artificial translation-initiation site was inserted. For protein production, *E. coli* BL21 (DE3) cells were transformed with the expression vector pQE60 bearing the cDNA from NLP_{Pya} (coding for amino acids 1–213), grown to an OD_{600} of 0.6 and induced with 1 m*M* IPTG for 8 h at 310 K. The construct included six histidine residues at the C-terminus. The sedimented cells were resuspended in 8 *M* urea, 0.1 *M* NaH_2PO_4, 0.01 *M* Tris–HCl pH 8.0 and disrupted by sonification. After centrifugation at 50 000*g* for 60 min, the protein was purified *via* a batch-purification protocol employing the C-terminal His_6 tag. The loaded Ni–IMAC matrix (Ni–NTA agarose, Qiagen, Hilden, Germany) was washed three times with 0.1 *M* NaH_2PO_4, 0.02 *M* imidazole, 0.01 *M* Tris–HCl pH 6.3 containing decreasing urea concentrations of 2, 0.5 and 0.1 *M*. After a final wash step with 0.05 *M* Na_2HPO_4/NaH_2PO_4 pH 8.0, 0.3 *M* NaCl, 0.3 *M* imidazole, the protein was eluted with 6 *M* guanidine–HCl and 0.2 *M* acetic acid. The protein was dialyzed in four steps against distilled water and adjusted to pH 6 in 0.05 m*M* Tris–MES. A subsequent centrifugation at 75 000*g* for 30 min removed any insoluble protein. The same protocol was used for the purification of the SeMet-labelled protein. The protein was concentrated in the above buffer using centrifugal devices and stored at 193 K.

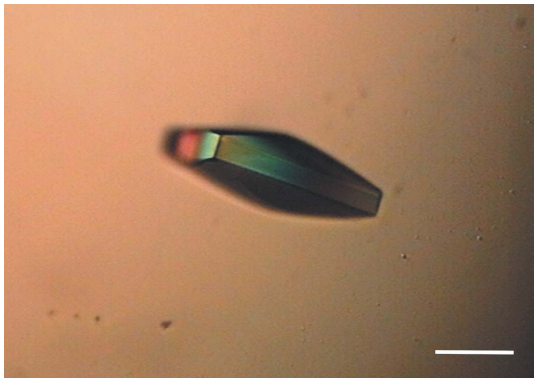

Figure 1
Native crystal of NLP_{Pya} grown after pre-precipitation with 20% PEG 4000, 0.5 *M* $MgCl_2$, 0.1 *M* Tris–HCl pH 9.0, 5% methanol. This crystal diffracted to 1.35 Å resolution. The scale bar is 100 µm in length.

2.2. Crystallization

In order to crystallize NLP_{Pya}, initial screenings employing Crystal Screen, Crystal Screen 2 and Crystal Screen Lite from Hampton Research were performed at 293 K using vapour diffusion. The protein concentrations in the setups were 25, 12.5 and 5 mg ml^{-1}; 1 µl protein solution was manually mixed with 1 µl reservoir solution in hanging drops. The hanging drops were equilibrated against reservoirs with a volume of 1 ml. Immediate heavy precipitation was observed in nearly every condition even at the lowest protein concentration. After two weeks, small crystals appeared in the heavy precipitate in one condition (Crystal Screen condition No. 6; 0.1 *M* Tris–HCl pH 8.5, 0.2 *M* $MgCl_2$, 30% PEG 4000). By lowering the PEG 4000 concentration to 20%, raising the $MgCl_2$ concentration to 0.5 *M* and the pH to 9.0 and including 5% methanol as an additive in new drops, crystal growth was improved slightly but was still unsatisfactory. These crystals did not grow beyond 20 × 20 × 10 µm and were of poor quality as judged by light microscopy. By performing a pre-precipitation with highly concentrated protein (50 mg ml^{-1}) with this reservoir solution and subsequent centrifugation at 16 000*g* for 20 min at room temperature, a supernatant was obtained that produced crystals of fine quality. To this end, equal volumes (typically 100 µl) of protein solution and reservoir solution (20% PEG 4000, 0.5 *M* $MgCl_2$, 0.1 *M* Tris–HCl pH 9.0, 5% methanol) were mixed. The resulting supernatant after the centrifugation was set up as hanging drops without further addition of reservoir solution and equilibrated against reservoir solution (2 µl drops of mixed supernatant, 1 ml of reservoir solution in the reservoir). The protein concentration in the supernatant after this precipitation procedure was about 5–8 mg ml^{-1}. These crystals grew to dimensions of 200 × 200 × 100 µm (Fig. 1) within a week. After soaking in reservoir solution supplemented with methanol to 20%, the crystals were cryocooled in liquid nitrogen for X-ray data collection at 100 K.

Since NLP_{Pya} is the first member of the NLP family that has been crystallized and no similar protein structure could be found in the Protein Data Bank, the phasing problem had to be solved experimentally. To this end, we attempted to obtain crystals of the SeMet-

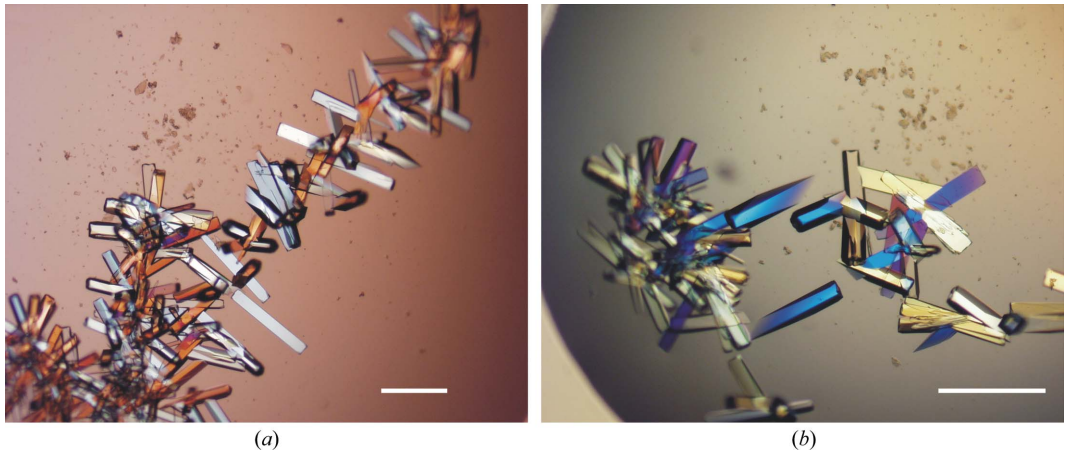

(*a*) (*b*)

Figure 2
(*a*) Streak-seeded native crystals of NLP_{Pya} grown after pre-precipitation with 0.1 *M* HEPES–NaOH pH 8.0, 5.0 *M* NaCl. These native crystals diffracted to 1.9 Å resolution, but no data sets from these crystals were used for structure elucidation. (*b*) Streak-seeded SeMet-labelled NLP_{Pya} crystals that diffracted to 2.1 Å resolution. These were used for experimental phasing. The scale bars are 100 µm in length.

Table 1
Data-collection statistics.

Values in parentheses are for the highest resolution shell.

		SeMet NLP_{Pya}		
	NLP_{Pya}	Peak	Inflection	High-energy remote
Wavelength (Å)	1.0052	0.97644	0.97936	0.96862
Resolution (Å)	20–1.35 (1.45–1.35)	15–2.1 (2.2–2.1)		
Space group	*C*222	$P4_32_12$		
Unit-cell parameters (Å)	$a = 69.6$, $b = 140.9$, $c = 49.6$	$a = b = 53.1$, $c = 175.3$		
V_M (Å^3 Da^{-1})	2.53	2.60		
Solvent content (%)	51.5	52.3		
Unique reflections	53077 (10317)	27873 (3624)		
Average redundancy	3.8 (3.1)	7.1 (7.0)	5.2 (5.1)	5.2 (5.1)
$\langle I/\sigma(I)\rangle$	16.9 (4.2)	15.2 (6.0)	12.7 (3.8)	14.5 (5.3)
Completeness (%)	98.3 (92.1)	99.5 (99.0)	99.5 (99.0)	99.5 (99.0)
Wilson *B* factor (Å^2)	16.6	38.5	36.8	38.2
R_{merge}† (%)	5.0 (28.1)	8.4 (36.1)	8.3 (37.7)	7.2 (33.8)

† $\sum_{hkl}\sum_i |I_i(hkl) - \langle I(hkl)\rangle| / \sum_{hkl}\sum_i I_i(hkl)$, where $I_i(hkl)$ is the scaled observed intensity of the *i*th symmetry-related observation of reflection *hkl* and $\langle I(hkl)\rangle$ is the mean value.

labelled derivative of NLP_{Pya}. This was not successful as the SeMet-labelled protein did not crystallize under the conditions used for the native protein. In addition, the alternative approach to obtain derivative crystals by cocrystallization or soaking with heavy atoms failed, despite the collection of 18 different derivative data sets. Among these, we tried several Au, Pt, Hg, Cs, U and Ag derivatives as well as lanthanides such as Eu, Sm, Gd, Ho, Yb and Ta. Interestingly, the soaked or cocrystallized crystals did not display reduced diffraction quality. This fact coincided with our inability to identify heavy-atom sites in any of the crystals for which data sets had been collected.

To find new crystallization conditions which might be more amenable for experimental phasing, we therefore repeated the screen with Crystal Screen and Crystal Screen 2 from Hampton Research at 293 K, employing the aforementioned pre-precipitation method. 5 µl protein solution (50 mg ml^{-1}) was mixed with 5 µl of each single condition from the screens and then centrifuged for 20 min (16 000*g*) at room temperature. 2 µl of the resulting supernatant was used to set up the hanging drops (without further addition of the crystal condition from the screens) and equilibrated against a reservoir volume of 1 ml. This time numerous crystallization conditions were identified. In condition No. 36 of Crystal Screen 2 (0.1 *M* HEPES–NaOH pH 7.5, 4.3 *M* NaCl) promising but somewhat crooked crystals appeared that could be optimized to single crystals by adding DTT (2%) and raising the pH to 8.0 and the NaCl concentration to 5.0 *M*. Controlled growth of these crystals was induced by streak-seeding (Fig. 2*a*). Under these conditions (pre-precipitation, 0.1 *M* HEPES–NaOH pH 8.0, 5.0 *M* NaCl and streak-seeding with native crystals) the SeMet-labelled protein also crystallized readily (Fig. 2*b*).

2.3. Data collection

Prior to data collection, crystals were cryocooled by direct transfer into liquid nitrogen. For cryoprotection of the native crystals, the methanol concentration was raised to 20%. In the case of the SeMet crystals the NaCl concentration of 5.0 *M* was already cryoprotective.

A native data set was collected from an optimized NLP_{Pya} crystal grown in 20% PEG 4000, 0.5 *M* $MgCl_2$, 0.1 *M* Tris–HCl pH 9.0 and 5% methanol at 100 K on ESRF beamline ID-23 at a wavelength of 1.0052 Å using a MAR 225 CCD detector. The crystal-to-detector distance was 126 mm, the oscillation range was 1.0° and 99 frames of data were collected.

Data were indexed, integrated and scaled with the *XDS* package (Kabsch, 1993). The crystals diffracted to a maximal resolution of about 1.35 Å (Table 1) and a check for possible systematic absences revealed that the crystals belonged to space group *C*222, with one monomer per asymmetric unit. This corresponds to a V_M value of 2.53 Å^3 Da^{-1} (Matthews, 1968) and a solvent content of 60%.

We also performed a three-wavelength MAD experiment using one SeMet-labelled crystal grown in 0.1 *M* HEPES–NaOH pH 8.0, 5.0 *M* NaCl at 100 K on SLS beamline X10SA (PXII) using a MAR 225 CCD detector. The crystal-to-detector distances were 200 mm for all three wavelengths and the oscillation range for all MAD data sets was 0.75°. The wavelength-dependent data sets were collected in the order peak, inflection and high-energy remote of the selenium absorption edge. The MAD data were also indexed, integrated and scaled with the *XDS* package (Kabsch, 1993). Data-set statistics are given in Table 1. The derivative search was performed with the program *SnB* and experimental phasing was performed with *PHASES* using the *BnP* (v.1.02) interface (Weeks & Miller, 1999). All four possible selenium sites could be found. Electron-density interpretation and structure refinement are in progress.

The authors are grateful to the staff of the Swiss Light Source (SLS), Villigen, Switzerland for technical support and Ilme Schlichting, Wulf Blankenfeldt, Andrea Scrima and Nils Schrader for data collection.

References

Amsellem, Z., Cohen, B. A. & Gressel, J. (2002). *Nature Biotechnol.* **20**, 1035–1039.
Bailey, B. (1995). *Phytopathology*, **85**, 1250–1255.
Chisholm, S. T., Coaker, G., Day, B. & Staskawicz, B. J. (2006). *Cell*, **124**, 803–814.
Gijzen, M. & Nürnberger, T. (2006). *Phytochemistry*, **67**, 1800–1807.
Kabsch, W. (1993). *J. Appl. Cryst.* **26**, 795–800.
Matthews, B. W. (1968). *J. Mol. Biol.* **33**, 491–497.
Mattinen, L., Tshuikina, M., Mäe, A. & Pirhonen, M. (2004). *Mol. Plant Microbe Interact.* **17**, 1366–1375.
Nürnberger, T., Brunner, F., Kemmerling, B. & Piater, L. (2004). *Immunol. Rev.* **198**, 249–266.
Qutob, D. *et al.* (2006). *Plant Cell*, **18**, 3721–3744.
Veit, S., Wörle, J. M., Nürnberger, T., Koch, W. & Seitz, H. U. (2001). *Plant Physiol.* **127**, 832–841.
Weeks, C. M. & Miller, R. (1999). *J. Appl. Cryst.* **32**, 120–124.
Zipfel, C., Robatzek, S., Navarro, L., Oakeley, E. J., Jones, J. D., Felix, G. & Boller, T. (2004). *Nature (London)*, **428**, 764–767.